Tuning of titanium dioxide surface energy levels by self-assembled monolayers for optoelectronic applications

Thierry Pauporté, Tao Zhu, Selina Olthof

Please cite this paper as : T Pauporté, T. Zhu, S. Olthof, Tuning of Titanium Dioxide Surface Energy Levels by Self-Assembled Monolayers for Optoelectronic Applications. Proc. SPIE, 12422 (2023) 1242208. https://doi.org/10.1117/12.2647864

Tuning of Titanium Dioxide Surface Energy Levels by Self-Assembled Monolayers for Optoelectronic Applications

Thierry PAUPORTÉ*[a], Tao ZHU[a], Selina OLTHOF[b]

[a] Chimie ParisTech, PSL University, CNRS, Institut de Recherche de Chimie Paris (IRCP), 11 rue P. et M. Curie, F-75005 Paris, France. [b] University of Cologne, Department of Chemistry, Greinstrasse 4-6, 50939 Cologne, Germany.
*Email : thierry.pauporte@chimieparistech.psl.eu

ABSTRACT

Tailoring the surface work function and/or surface functional group of oxide active layers in an optoelectronic device is an important means for performance improvement. One way to proceed is to adsorb molecules with varying dipole moment strength and sign. We report on the surface modification of mesoporous TiO_2 using different self-assembled monolayers (SAMs) of acids. The energetics at the interface have been determined using a series of photoelectron spectroscopy techniques (UPS, IPES, XPS). We have shown that the observed changes in work function is correlated to the dipole moments of the respective acids, calculated by density functional theory. This interfacial engineering approach can be used to control the charge extraction from an optoelectronic device. A novel approach is proposed for boosting the performances of self-powered photodetectors. Visible-blind UVA photodetectors have been built by combining a mesoporous TiO_2 layer with a Spiro-OMeTAD layer. SAMs interlayer induces a step in the vacuum energy, the formed dipole field dramatically affects the charge transfer and then the photocurrent/photoresponse of the device. The effect of para-substituted benzoic acids and β-alanine on the functioning of triple cation perovskite solar cells is then developed. We show then a best improvement for 4-chlorobenzoic acid SAMs which is due to the reduction of interfacial states, to the improvement of the quality of the perovskite material and to a better structural continuity.

Keywords: Self-assembled monolayers, anatase TiO_2, benzoic acids, photoelectron spectroscopies, self-powered Photodetector, UV-A, perovskite solar cells, density functional theory.

1. INTRODUCTION

Semiconductor oxide layers are widely employed in emerging optoelectronic devices. Their surface can be modified through self-assembled monolayers (SAMs) of organic molecules of various dipole moment strength and sign for the improvement of the interface and contact with semiconductor overlayers to increase the performances.[1-4] Important applications encompass UV-photodetectors,[5-9] organic photovoltaics (OPV) [10,11] and perovskite solar cells (PSC).[12-16] Anatase phase compact-TiO_2 (c-TiO_2) and mesoporous-TiO_2 (meso-TiO_2) bilayers are employed as large bandgap (3.2 eV) selective contact in various optoelectronic devices.[17,18] Energy level adjustment and engineering can be operated by adsorbing monolayers of organic molecules which self-assemble onto the surface. Acid compounds are of great interest since they bind onto the oxide surface by means of their acid function. These SAMs induce energetic changes related to their dipole moment and intrinsic energy levels (work function (W_f), HOMO/LUMO…).[1] It results in a modification of the band alignment with adjacent layers in opto-electronic devices. Spectroscopic techniques such as the photoelectron-based ones allow to fully draw the energy diagrams of these systems and the investigation of SAMs effects. The acid group can also play a positive role by passivating surface defects.

Here, we have experimentally investigated the changes induced by four different acid molecules on the surface properties of TiO_2. The investigated acids are para-substituted benzoic acid derivatives: 4-chlorobenzoic acid (CBA), 4-methoxy benzoic acid (MBA), and 4-nitro benzoic acid (NBA). Additionally, β-alanine (also called 3-aminopropanoic acid and noted ALA), an amino-acid, is also investigated. We first show how the energy band diagram of the systems is changed by the presence of these SAMs composed of molecules of various dipole moment strength and sign. Then we

Please cite this paper as : T Pauporté, T. Zhu, S. Olthof, Tuning of Titanium Dioxide Surface Energy Levels by Self-Assembled Monolayers for Optoelectronic Applications. Proc. SPIE, 12422 (2023) 1242208.
https://doi.org/10.1117/12.2647864

develop their application to UV-A self-powered photodetector driven by built-in electric field. Finally, the interest of SAMs at the interface between the electron transporting layer and the perovskite layer is emphasized for solar cell application.

2. RESULTS AND DISCUSSION

2.1 Photoelectron Spectroscopy investigations

We prepared TiO_2 layers on glass/FTO substrate, a popular substrate in optoelectronics. First a compact TiO_2 layer (c-TiO_2) was grown by spray pyrolysis at 450°C. Then a mesoporous film (meso-TiO_2) composed of anatase TiO_2 nanoparticles with a mean size of 30 nm was deposited by spin coating. The thickness was 20 nm for the former and was 120-150 nm for the latter. Then SAMs of CBA, NBA, MBA and ALA were formed. These acids were dissolved in methanol. The solution was dropped onto the meso-TiO_2 layer, let to react and then spin-coated. The samples were annealed at 100°C on a hotplate for 10 min. They were finally rinsed with pure methanol.

The samples were first investigated by ultraviolet photoelectron spectroscopy (UPS) that allowed us to extract W_f, the HOMO and the ionization energy (IE) of the samples.[1] The work function (W_f) was deduced from the high energy cutoff using the relationship: $W_f = 21.22\ eV - E_{cutoff}$ (eV), 21.22 eV being the energy of the UV photons. As the cutoff region UPS signal reflects the properties of the topmost layer, this parameter is affected by the SAMs which modify the position of the vacuum level.

To access the HOMO energies of SAMs, the spectra were treated by subtracting the UPS signal of the pristine meso-TiO_2 sample. The intensity of the meso-TiO_2 signal was adjusted to give the best result after an accurate subtraction, judged from the gaussian shape symmetry of the resulting spectra. It gave E_{HOMO}, the HOMO onset energy versus E_F. The ionization energy, IE, is the sum $E_{HOMO} + W_f$. UPS also provided us the valence band energy of TiO_2 (VB_{TiO2}) measured, from the low energy edge of the pristine sample, at 3.57 eV versus E_F.

Table 1. Energies of the SAMs/TiO_2 heterostructures extracted from the UPS, IPES and XPS measurements. The VB_{TiO2}, $E_{HOMO,SAM}$, CB_{TiO2}, $E_{B,TiO2}$ and values are given with respect to E_F.

Compound	$\mu_\perp$ **(D)**	***Wf*** **(eV)**	**VB_{TiO2} (eV)**	**$E_{HOMO,SAM}$ (eV)**	**CB_{TiO2} (eV)**	**IE / EA (eV)**	**$E_{B,TiO2}$ (eV)**
meso-TiO_2	0	3.8	3.57		0.15 eV	7.37 / 3.65	459.09
MBA	-0.50	3.69		3.44		7.13 / --	459.07
NBA	2.22	4.27		2.37		6.64 / --	458.89
CBA	0.89	4.08		3.00		7.08 / --	459.09
ALA	0.12	3.88		3.94		7.82 / --	459.13

Inverse photoelectron spectroscopy (IPES) was then employed to probe the conduction band (CB).[1] The bottom of CB was found at 0.15 eV above E_F for the pristine meso-TiO_2 sample. It is noteworthy that, due to noise, the LUMO of SAMs could not be investigated by IPES.

We found that W_f is deeply affected by the SAMs.[1] Compared to the pristine sample, we observed a lowering of ~110 mV for MBA. On the other hand, it exhibited an increase of 80 meV, 280 meV and 470 mV for ALA, CBA and NBA, respectively. The amplitude and the sign of these changes are perfectly correlated with the normal component of the dipole moment of the acid molecules calculated by density functional theory (DFT) in Ref.[4] The various energies extracted from the UPS, IPES and XPS studies are gathered in **Table 1**.

Please cite this paper as : T Pauporté, T. Zhu, S. Olthof, Tuning of Titanium Dioxide Surface Energy Levels by Self-Assembled Monolayers for Optoelectronic Applications. Proc. SPIE, 12422 (2023) 1242208.
https://doi.org/10.1117/12.2647864

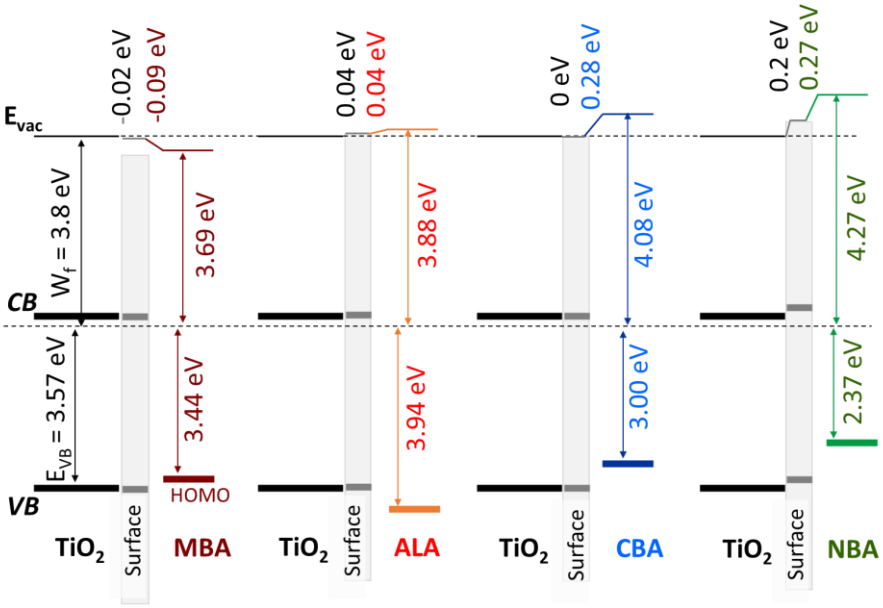

Figure 1. Energy band level diagram of TiO_2 surfaces treated by SAMs and compared to the pristine sample.(Adapted from Ref.[1]. Copyright 2022, AIP Publishing)

We have considered that the change in the vacuum level is due to the electric field across the SAMs layer. However, the electronic structure of the underlying anatase can be affected by the dipole. By measuring the x-ray photoelectron spectra (XPS) of Ti 2p core level signals, we found that its position was not significantly changed for MBA, CBA and ALA SAMs. Therefore, in this case, VB and CB of TiO_2 is the same in the bulk and at the surface (**Figure 1**). On the other hand, we found that NBA, which has the highest dipole moment, leads to a ~200 meV shift of the Ti 2p core level signal toward a lower binding energy. VB and CB of the TiO_2 bulk are shifted to a lower energy compared to the surface. The W_f shift is divided into two contributions: a core level one and a step in the local vacuum. In conclusion, UPS, IPES and XPS characterization allowed us to draw the full energy diagrams of the investigated systems shown in **Figure 1**. In so far as overlayers will keep the presented diagrams and energy trends, it can be clearly seen that ALA, CBA and NBA SAMs will be favorable to the electronic charge extraction and hole blocking in an optoelectronic device.

2.2 Application to UVA Photodetectors

Photodetectors (PDs) are used to convert an incident optical signal into an electrical one. Currently, detection of the optical signal at a wavelength in the ultraviolet (UV), visible, and infrared (IR) region is performed by distinct types of photodetectors. The efficient photodetection of ultra-violet (UV) electromagnetic radiations is attracting a large attention due to it utmost importance.[5-9] Systems have been designed for applications in environmental and biological analysis or monitoring, flame detection, military applications, geology detection, space communication, chemical and pharmaceutical analyses and industrial quality control. UVA, which wavelength ranges between 315 nm and 400 nm, can be directly detected by wide bandgap semiconductor-based heterostructures.

We have built a PD device in Ref.[9] by adding a Spiro-OMeTAD layer onto the previous described structure and by adding a back contact. The Spiro-OMeTAD was deposited from a solution by spin-coating and a gold back contact was thermally evaporated. The c-TiO_2/meso-TiO_2 bilayer was treated by the same SAMs as before, namely MBA, ALA, CBA and NBA. The Spiro-OMeTAD was employed without adding doping agent and additive to prevent any disturbance of the interface with the acid-modified TiO_2. We have observed initial S-shaped *J-V* curves. It has been assigned to the low conductivity of undoped Spiro-OMeTAD (3.10^7 S cm^{-1}).[19] It leads to a difficult charge extraction and charge accumulation occurs at the interface which enhances charge recombination. The device was stored then in air to get the stable classical *J-V* curve shape with high J_{sc}. Due to the oxidation reaction of SpiroOMeTAD by air oxygen:

$$\text{Spiro-OMeTAD} + O_2 \rightarrow \text{Spiro-OMeTAD}^{\bullet +} O_2^{\bullet -} \qquad (1)$$

Please cite this paper as : T Pauporté, T. Zhu, S. Olthof, Tuning of Titanium Dioxide Surface Energy Levels by Self-Assembled Monolayers for Optoelectronic Applications. Proc. SPIE, 12422 (2023) 1242208.
https://doi.org/10.1117/12.2647864

the molecular layer was p-type doped and its conductivity increased.

The PD was shown visible-blind because Spiro-OMeTAD is a large bandgap (3.0 eV) semiconductor in Ref.[19]. Moreover, once matured, under UVA-light shining (λ=365 nm), the PD current density at 0 V increased with the order MBA<ALA<Blank<CBA<NBA while the V_{oc} increased in the following order: NBA<CBA<Blank<ALA<MBA. We can explain this behavior based on the previous section characterizations and the effect of the dipole sign and strength of the modifiers on the vacuum level and energy diagram. The schematic energy diagrams are shown in **Figure 2**. The dipole moment convention sign here is positive for + to -. If $\mu_\perp > 0$, the vacuum energy level is shifted upward. This induces a favorable electric field for the electron extraction and enhances the current generated by the PD (**Figure 2a**). On the other hand, if $\mu_\perp < 0$, the electric field is unfavorable to the electron charge transfer and the PD current is lowered (**Figure 2c**). We can note that we found previously a slight positive increase in the vacuum level for ALA modifier (**Figure 1**). However, when employed in PD, ALA led to a J_{sc} lower than for the blank. It shows that for this modifier, the Spiro-OMeTAD has a great impact and change the interface properties. A special behavior was also observed for this molecular modifier by measuring the work function with a Kelvin probe since we found a higher W_f for the ALA-TiO_2 system compared to the pristine one.[9]

Due to the energy band shift, the V_{oc} variation is inverse. A dipole moment, and then an electric field, pointing toward the Spiro-OMeTAD layer lower the induced photovoltage (**Figure 2a**). On the other hand, a dipole moment, and then an electric field, pointing toward TiO_2 increases the induced photovoltage (**Figure 2c**). This phenomenon is clearly illustrated in **Figure 2.**

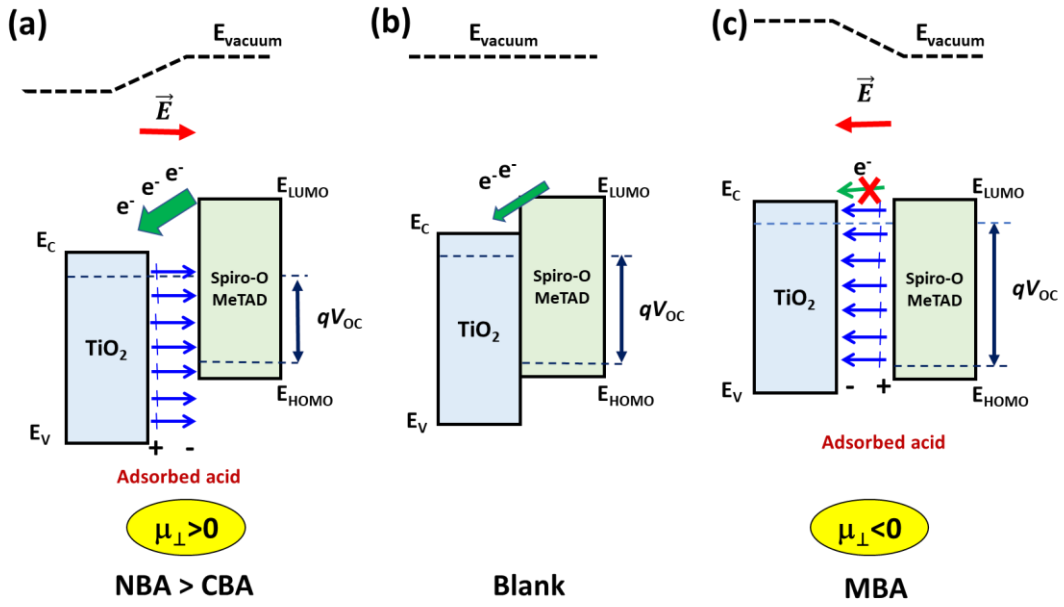

Figure 2. Schematic diagrams of the effect of interfacial dipole modifiers on the energy band level in TiO_2/Spiro-OMeTAD PD. (a) positive and (c) negative dipole component normal to the surface. (b) Blank without modifier.

The properties of NBA-modified and blank PDs were further characterized in Ref.[9]. The rectification ratio, which measures ratio between the dark current at +1V and -1V, was determined at 900 for the blank PD and 400 for the NBA-PD. Their sensitivity at 0V, which is the J_{light}/J_{dark} ratio, was determined at 1.2 10^4 and 2.3 10^4 for the NBA-PD at an irradiance of 23 mW.cm^{-2} and 47 mW.cm^{-2}, respectively (**Table 2**). The sensitivity of the pristine PD was lower at 0.92 10^4 and 2.0 10^4 at an irradiance of 23 mW.cm^{-2} and 47 mW.cm^{-2}, respectively. We also noted the significantly lower performance of the MBA device (**Table 2**) due to the negative dipolar moment and an electric field oriented toward the

Please cite this paper as : T Pauporté, T. Zhu, S. Olthof, Tuning of Titanium Dioxide Surface Energy Levels by Self-Assembled Monolayers for Optoelectronic Applications. Proc. SPIE, 12422 (2023) 1242208. https://doi.org/10.1117/12.2647864

TiO_2 layer (**Figure 2**). The external quantum efficiency (EQE) was measured at 21 % for the NBA-modified PD and 13.7 % for the blank. The responsivity is defined as :

$$R = \frac{EQE(\%)\lambda q}{hc} \qquad (2)$$

λ is the radiation wavelength, q is the elemental charge, h is the Planck constant and c the light velocity. NBA-modified PD achieved a responsivity maximum at 64 $mA.W^{-1}$ and its rejection ratio was 159. This PD also exhibited an excellent repeatability. Its rise and decay times were in the ms order. We also noted that the NBA SAMs had a strong beneficial effect on the stability of the device stored under ambient condition for several months. The measured J_{sc} was almost unchanged after a storage of 156 days.[9]

Table2. Photodetector sensitivity (J_{light}/J_{dark}) for pristime and SAMs modified devices at 0V for λ = 365 nm.

Irradiance	Blank	NBA	CBA	ALA	MBA
23 $mW.cm^{-2}$	9.2 10^3	1.2 10^4	8.9 10^4	1.6 10^4	5.1 10^3
47 $mW.cm^{-2}$	2.0 10^4	2.3 10^4	1.5 10^4	2.4 10^4	7.9 10^3

2.3 Application to perovskite solar cells.

Perovskite solar cells (PSCs) are based on halide perovskite (PVK) solar light absorbing layers. They have recently demonstrated high power conversion efficiency (PCE) and great potentials.[20-23] SAMs are of great interest to engineer interfaces in PSCs. They can induce many positive effects that will result in better device performances. They can improve the morphology of the halide perovskite layer, introduce a permanent molecular dipole moment normal to the surface and the generated electric field can favor the electron charge extraction toward the oxide electron transporting material. The carboxylic acid group can passivate trap state defects of the oxide layer, while the para-substituting functional group can also passivate perovskite defects. They can act as an insulating layer delaying the charge recombination. They can also act as a barrier between halide perovskite and the underlying layer to avoid undesired reactions.

To prepared PSC, in Ref.[12], we started from the structures presented in the section 2.1 on which, a halide perovskite layer, with composition $Cs_{0.08}FA_{0.80}MA_{0.12}Pb(I_{0.88}Br_{0.12})_3$, was deposited by spin-coating. Then, the device was completed by adding a layer of doped Spiro-OMeTAD containing dopants, prepared by spin-coating, and a gold counter-electrode deposited by thermal evaporation. Besides the previously investigated organic surface modifier, we also studied 4-bromobenzoic acid (BrBA) and 4-aminobenzoic acid (ABA). Our conclusion was that the best cells were produced using CBA.[12] PCEs higher than the control cells were obtained with CBA, BrBA and MBA modifiers. The performance of the ALA-modified cells was close to the control one. The stabilized PCE was 20.0 % for the control and 20.9 % for the CBA treated device.[12] The remarkable point was that CBA also improved cells prepared with $MAPbI_3$ PVK.

The order for the measured PSC J_{sc} was : NBA<ALA<blank<MBA<CBA. We noted that this order differs to a great extent from to the $\mu_\perp$ one.[12] Notably, NBA, which has the highest dipole moment, gave a poorly functioning solar cell while MBA with a negative dipole moment gave better results than the blank device. It shows that, in this system, $\mu_\perp$ is not the main parameter that leads to the improvement. By finely investigating the perovskite layers, we found that the modifiers have no significant influence on the morphology, on the diffraction peak intensity and on the grain size of the perovskite. Slow decay times (τ_{sl}) determined by time-resolved photoluminescence (TRPL) provided the following values 183 ns, 117 ns, 79 ns, 64 ns, and 18 ns, for CBA, MBA, blank, β-ALA and NBA cells, respectively. Therefore, there is a good correlation between the slow decay time and the cells J_{SC}. We found that the higher the former, the higher the latter. τ_{sl} reflects the quality of the halide perovskite material and high values means low quenching phenomena in the bulk. On the other hand, the fast decay time (τ_{fast}), that traduces the speed of charge injection to TiO_2, was the shortest for CBA (1.47 ns versus 1.62 ns for the control). Therefore, the charge transfer is better with CBA SAMs. We deduced that

Please cite this paper as : T Pauporté, T. Zhu, S. Olthof, Tuning of Titanium Dioxide Surface Energy Levels by Self-Assembled Monolayers for Optoelectronic Applications. Proc. SPIE, 12422 (2023) 1242208.
https://doi.org/10.1117/12.2647864

perovskite formed on the CBA/TiO_2, and in a less extent, on the MBA/TiO_2 had a better structural and interfacial qualities than the pristine heterostructure.

Finally, the best structure with CBA was modelled by DFT in Ref.[4]. After geometry optimization, we found that the presence of chloride enables a stable bonding with the perovskite (via Pb-Cl) and the building of an organized CBA-TiO_2 interface. The computed density of states shows that the intermediate CBA induces a favorable band alignment that enable the efficient electron transfer between the perovskite and TiO_2. Calculations reveal a very efficient, almost quantitative, charge transfer between the PVK and TiO_2 calculated at 99.94%.[4]

CONCLUSION

In the present paper, we have fully described the electronic structure and band energy diagrams of mesoporous anatase TiO_2 layer modified by organic acids, especially benzoic acid derivatives, self-assembled onto their surface. We have shown that they allow the fine tuning of their energy properties, especially of the work function. We have then illustrated how these properties can be exploited to boost the performance of a self-powered UVA photodetector. Then we have shown that the effect of SAMs on PSCs is more complex. Indeed, in this case, SAMs act as an intermediate between TiO_2 and the perovskite layer. They play an important connection role. The chloride derivative led to stable bonding with the perovskite and to the building of an organized interface. In PSCs, SAMs have a great influence on the interfacial continuity, as well as on interfacial and bulk defect reduction.

REFERENCES

[1] T. Zhu, T., S. Olthof, S., Th. Pauporté, T., "Titanium dioxide surface energy levels tuning by self-assembled monolayers." Appl. Phys. Lett. 121, 141602 (2022).
[2] Hu, T., Becker, T., Pourdavoud, N., Zhao, J., Brinkmann, K. O., Heiderhoff, R., Gahlmann, T., Huang, Z., Olthof, S., Meerholz, K., Többens, D., "Indium-free perovskite solar cells enabled by impermeable tin-oxide electron extraction layers." Adv. Mater. 29, 1606656 (2017).
[3] Lim, K.G., Ahn, S., Lee, T.W., "Energy level alignment of dipolar interface layer in organic and hybrid perovskite solar cells." J. Mater. Chem. C 6, 2915-2924 (2018).
[4] J. Su, J., T. Zhu, T., Th Pauporté, T., I. Ciofini, I., F. Labat, F., "Improving the heterointerface in hybrid organic-inorganic perovskite solar cells by surface engineering: Insights from periodic hybrid density functional theory calculations". J. Comput. Chem. 41, 1740–1747 (2020).
[5] Al Fattah, M.F., Khan, A.A., Anabestani, H., Rana, M.M., Rassel, S., Therrien, J., Ban, D.Y., "Sensing of ultraviolet light: a transition from conventional to self-powered photodetector." Nanoscale 13, 15526-15551 (2021).
[6] Sang, L., Liao, M., Sumiya, M., "A Comprehensive review of semiconductor ultraviolet photodetectors: From thin film to one-dimensional nanostructures." Sensors 13, 10482 (2013).
[7] Alaie, Z., Mohamad Nejad, S., Yousefi, M.H., "Recent advances in ultraviolet photodetectors." Sci. Semiconductor Processing 29, 16 (2015).
[9] Zhu, T., Su, J., Alvarez, J., Lefèvre, G., Labat, F., Ciofini, I., Pauporté, T., "Response enhancement of self-powered visible-blind UV photodetectors by nanostructured heterointerface engineering." Adv. Funct. Mater. 29, 1903981 (2019).
[10] Kırbıyık, Ç., Kara, D.A., Kara, K., Büyükçelebi, S., Yiğit, M.Z., Can, M., Kuş, M., "Improving the performance of inverted polymer solar cells through modification of compact TiO_2 layer by different boronic acid functionalized self-assembled monolayers." Appl. Surf. Sci. 479, 177–184 (2019).
[11] Lim, K.-G., Ahn, S., Lee, T.-W., "Energy level alignment of dipolar interface layer in organic and hybrid perovskite solar cells." J. Mater. Chem. C 6, 2915–2924 (2018).
[12] Zhu, T., Su, J., Labat, F., Ciofini, I., Pauporté, T., "Interfacial engineering through chloride-functionalized self-assembled monolayer for high efficiency perovskite solar cells." ACS Appl. Mater Interfaces 12, 744-752 (2020).

Please cite this paper as : T Pauporté, T. Zhu, S. Olthof, Tuning of Titanium Dioxide Surface Energy Levels by Self-Assembled Monolayers for Optoelectronic Applications. Proc. SPIE, 12422 (2023) 1242208.
https://doi.org/10.1117/12.2647864

[13] Ogomi, Y., Morita, A., Tsukamoto, S., Saitho, T. Shen, Q., Toyoda, T., Yoshino, K., Pandey,S.S., Ma, T., Hayase, S., "All-solid perovskite solar cells with HOCO-R-NH_3^+ I^- anchor-group inserted between porous titania and perovskite." J. Phys. Chem. C 118, 16651–16659 (2014).

[14] Li, B., Chen, Y., Liang, Z., Gao, D., Huang, W., "Interfacial engineering by using self-assembled monolayer in mesoporous perovskite solar cell." RSC Adv. 5, 94290–94295 (2015).

[15] Liu, L., Mei, A., Liu, T., Jiang, P., Sheng, Y., Zhang, Han, "Fully printable mesoscopic perovskite solar cells with organic silane self-assembled monolayer." J. Am. Chem. Soc. 137, 1790–1793 (2015).

[16] Olthof, S., Meerholz, K., "Substrate-dependent electronic structure and film formation of $MAPbI_3$ perovskites." Sci. Rep. 7, 40267 (2017).

[17] Magne, C., Dufour, F., Labat, F., Lancel, G., Durupthy, O., Cassaignon, S., Pauporté, T., "Effects of TiO_2 nanoparticle polymorphism on dye-sensitized solar cell photovoltaic properties." J. Photochem. Photobiol. A, 232, 22-31 (2012).

[18] Wang, P., Shao, Z., Ulfa, M., Pauporté, T., "Insights into the hole blocking layer effect on the perovskite solar cell performance and impedance response." J. Phys. Chem. C, 121, 9131–9141 (2017).

[19] Ulfa, M, Pauporté, T., Bui,T.T. Goubard, F., "Impact of organic hole transporting material and doping on the electrical response of perovskite solar cells." J. Phys. Chem. C 122, 11651−11658 (2018).

[20] Li, M., Li, H., Q. Zhuang, Q., D. He, D., B. Liu, B., C. Chen, C., M. Jiang, M., S. Xu, S., S. Zheng, S., B. Zhang, B., Th. Pauporté, T., Z. Zang, Z., J. Chen, J., "Stabilizing perovskite precursor by synergy of functional groups for NiOx-based inverted solar cells with 23.5% efficiency." Angew. Chem. Int. Ed., 61, e202206914 (2022).

[21] Zheng, D., Zhu, T., Yan, Y., Pauporté, T., "Controlling the formation process of methylammonium-free halide perovskite films for a homogeneous incorporation of alkali metal cations beneficial to solar cell performances." Adv. Energy Mater., 12, 2103618 (2022).

[22] Leblanc, A., Mercier, N., Allain, M., Dittmer,J., Fernandez, V., Pauporté, T., "Lead and iodide deficient MAPI, d-MAPI: the bridge between 2D and 3D hybrid perovskites." Angew. Chem. Int. Ed., 56 16067 –16072 (2017).

[23] Choi, K, Choi, H., Min, J., Kim, T., Kim, D., Son, S.Y., Kim, G.W., Choi, J., Park, T., "A short review on interface engineering of perovskite solar cells: A self-assembled monolayer and its roles." Sol. RRL 1900251 (2019).